

Control of Thermal Flow in Machine Tools Using Shape Memory Alloys

Reimund Neugebauer, Welf-Guntram Drossel, André Bucht, Christoph Ohsenbrügge

Abstract—In this paper the authors propose and verify an approach to control heat flow in machine tool components. Thermal deformations are a main aspect that affects the accuracy of machining. Due to goals of energy efficiency, thermal basic loads should be reduced. This leads to inhomogeneous and time variant temperature profiles. To counteract these negative consequences, material with high melting enthalpy is used as a method for thermal stabilization. The increased thermal capacity slows down the transient thermal behavior. To account for the delayed thermal equilibrium, a control mechanism for thermal flow is introduced. By varying a gap in a heat flow path the thermal resistance of an assembly can be controlled. This mechanism is evaluated in two experimental setups. First to validate the ability to control the thermal resistance and second to prove the possibility of a self-sufficient option based on the self-sensing abilities of thermal shape memory alloys.

Keywords—energy-efficiency, heat transfer path, MT thermal stability, thermal shape memory alloy

I. INTRODUCTION

THERMAL deformation has a large impact on machining accuracy. Inhomogeneous heat dissipation leads to a shift at the tool centre point (TCP) and therefore a reduced achievable precision (up to 75% of the total error are attributed to thermal deformation [1]). As long as the machine operates in its thermal equilibrium, an active correction of thermally induced errors is possible by implementing suitable control algorithms or using thermo-symmetrical design [2], [3], [4]. In state-of-the-art machine tools the actuators as well as the coolant/lubricant circuit dissipate a constant heat flow as a basic load that is crucial for the stabilization of the thermo-elastic behavior of the machine. This basic load is maintained both in operation and in stand-by. Especially in productive processes with high metal removal rates and high accuracy requirements they are close to being indispensable.

In the context of energy efficiency these basic loads are looked at as potentially avoidable since they are not directly contributing to chip formation. The well-directed deactivation of these basic loads offers potential for improvements regarding the energy balance [5], [6]. But this conflicts with the effect of thermal stabilization. As a result of the deactivation, a time-varying temperature-field occurs that complicates a pure control-driven correction of the deviation of the TCP. The “SFB/Transregio 96” special research centre has the goal to

R. Neugebauer, W-G. Drossel and A. Bucht are with Fraunhofer Institute for Machine Tools and Forming Technology IWU, Reichenhainer Strae 88, 09126 Chemnitz, Germany.

C. Ohsenbrügge is with Institute for Machine Tools and Production Processes, Chemnitz University of Technology, Reichenhainer Strae 70, 09107 Chemnitz, Germany

Manuscript received April 19, 2005; revised January 11, 2007.

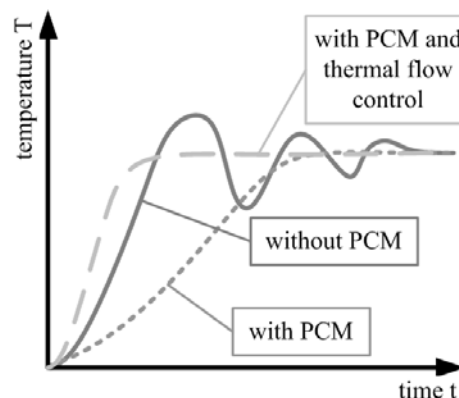


Fig. 1. Effect of thermal storage and thermal flow control on a temperature profile

resolve the conflict between high machining accuracy, energy efficiency and productivity by researching solutions to reduce the effect of thermo-elastic deformations on the TCP [7].

A. Thermal Buffer as Stabilizing Mechanism

While the control-driven correction is one investigated option, another one is the compensation of thermal effects by directly influencing the thermal flows within components. An homogenization of the temperature field is achieved by selectively using additional thermal capacities. Due to its high melting enthalpy, phase change material (PCM) is able to store large amounts of thermal energy in a small temperature interval [8], [9]. The addition of PCM leads to damping of fluctuations in heat input. A similar approach was also investigated in [10].

With an increased thermal inertia, a component will stay longer in thermal equilibrium under the influence of an unsteady thermal flow. Obviously a high thermal capacity will result in a changed transient behavior of the structure. The warm-up time will increase and the thermal equilibrium will be delayed. To compensate for that disadvantage the authors propose a mechanism to actively control the thermal coupling of the additional thermal capacity to the component. Fig. 1 shows the qualitative effect of this principle. While the uninfluenced profile exhibits a varying thermal behavior, the addition of PCM will smooth the deviations and the active control will lead to a faster rise towards the equilibrium temperature.

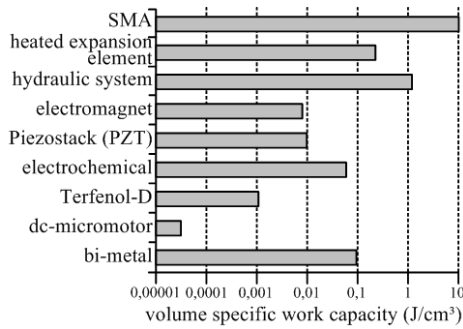


Fig. 2. Comparison of volume specific working capacities [11]

II. ACTIVE CONTROL OF THERMAL FLOW

The proposed approach to actively control the heat flow from a component into a thermal storage is based on the effect of opening and closing gaps in a transfer path. Since air has a thermal conductivity of approximately $\lambda_{air} = 25.42 \cdot 10^{-3} \text{ W/m}\cdot\text{K}$ at 20°C it acts as an isolator. Therefore, the thermal resistance of the assembly can be adjusted by reducing or increasing an air-filled gap.

A. Shape Memory Alloys

To avoid the consumption of energy for altering the thermal resistance, the mechanism should be self-sufficient. Considering that the thermal resistance of the assembly should alter depending on the temperature of the component, the usage of the thermal field as control parameter is desirable. Thermal shape memory alloys (SMA) allow this mechanical actuation based on thermal activation by using the one-way shape memory effect. SMAs exhibit a very large volume specific work capacity in comparison to other actuator-principles (see fig. 2). This allows for a lightweight and highly integrated solution.

Summing up an actuator based on the thermal shape memory effect will mechanically alter the state of an air gap in a thermal flow path from a component to a thermal storage. In initial state the gap will be open in order to allow a fast warm-up of the component into operating temperature. Upon reaching a certain temperature the actuator should be activated and consequently it closes the gap and reduces the thermal resistance. If temperature drops below a certain point the gap will be opened and thereby the thermal storage will be separated from the component again. Two approaches for realization of this mechanism are proposed: a compression spring made of SMA that is activated by joule heating and a leaf spring that is thermally coupled to the component to be regulated. The setup with the leaf spring directly uses the thermal energy of the heat source and thus provides a self-sufficient approach. To allow for a repeatable process the SMA based actuator needs a counterpart to force it back into its original shape. In this work the authors use an extrinsic force realized by a second spring (or leaf spring) made from steel.

B. Active Spring vs Passive Spring

A compression spring made of SMA will change its spring rate depending on its phase [12]. On the one hand this is

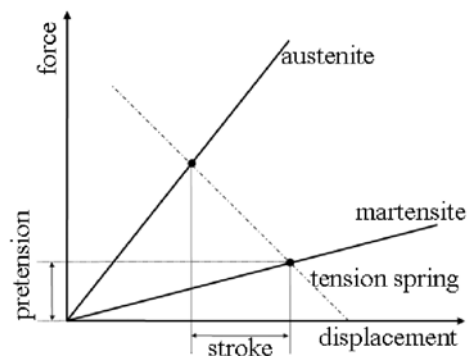


Fig. 3. Dimensioning of an actuator system with SMA and conventional tension spring

attributed to the different Young's modulus of the martensitic and the austenitic phases and on the other hand to the trained shape. A conventional tension spring acts as a counter force. The two springs and the pretension of both have to be designed to comply with the requirements in regard to resulting stroke and contact pressure as seen in fig. 3. Heating of the active spring is realized by joule heating. This setup is sufficient to demonstrate the basic mechanism of an adjustable thermal resistance but as it needs active control a second design was investigated.

C. Active Leaf Spring vs Passive Spring

To prove the feasibility of a self-sufficient mechanism directly using the energy of the source of heat, a slightly different setup is necessary. Considering the geometry of a compression spring it poses a challenge to couple it thermally to the heat source in order to heat it with thermal energy taken from the process. As an alternative a leaf spring made of SMA was selected. One of its ends is connected to the component allowing a large contact area to transmit heat. A radius was trained into the SMA sheet to achieve an active bending upon activation. As opposing force a leaf spring made of spring steel is used in antagonistic configuration. The conventional leaf spring is connected to the component with an isolating layer in between to not further increase the thermal capacity of the component.

III. EXPERIMENTAL SETUP

Experimental verification of the proposed control mechanism for thermal flow was carried out. The basis of the experiment was a copper beam where one end was heated with a heating cartridge, the other end was connected to a cooling circuit. A wedge was cut out from the middle of the beam to create the variable gap as seen in fig. 4. Its point angle is large enough to prevent static friction. The wedge is connected to the active spring and to the passive conventional spring. The active spring was designed so it will provide enough force in its activated state to push the wedge into the gap and thereby reducing the thermal resistance of the assembly. If the SMA cools down again its spring force will lower and the steel spring moves the wedge out of the gap.

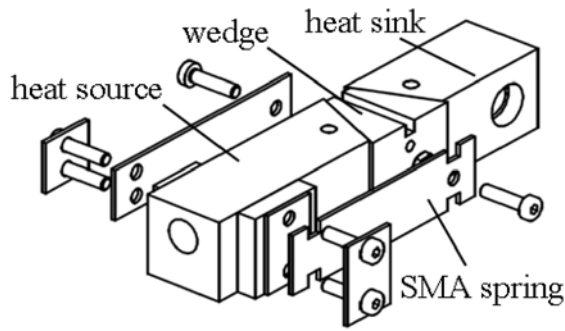


Fig. 4. Experimental setup

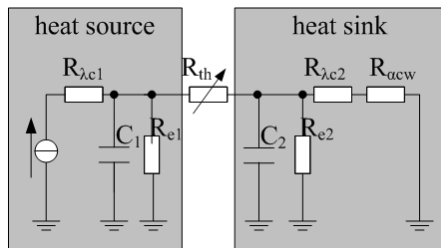


Fig. 5. Overall thermal network

In order to reduce the influence of thermal leakage current the assembly is enclosed in insulation. The thermal resistance of the contact areas (wedge to beam) was reduced by using thermal compound.

A. Thermodynamic Modeling

The possible performance of the approach was determined using a thermal network in analogy to electrical networks. It consists of three main parts: The part of the copper beam containing the heat cartridge, called heat source, the middle part covering the air gap and the wedge and the third part connected to the cooling circuit called heat sink. Both heat source and heat sink are composed of the thermal resistance of the copper ($R_{\lambda c1}$, $R_{\lambda c2}$), the resistance towards the environment (R_{e1} , R_{e2}) and a thermal capacity (C_1 , C_2).

While two different setups were developed both can be described with the same thermal network for the steady-state case. Only the mechanism for activation of the SMA-actuator and its transient behavior differs. Fig. 5 shows the global thermal schematic with the heat source and heat sink.

While the thermal resistance of the heat source and the heat sink will be assumed to be constant, the description of the middle part (R_{th}) is the main task of the modeling. A graphic representation of the two possible states is shown in fig. 6. In closed state the thermal resistance consists of the thermal conductance resistance from the copper of the wedge ($R_{\lambda c}$) and the thermal contact resistance between the wedge and the remaining beam (R_{cc}). In open state the air gaps are the central factor. The description of each gap is constructed out of three resistances: The two R_{acc} describe the heat transfer resistance from the copper to air and $R_{\lambda a}$ is the thermal resistance of the air. It is variable and depends on the width of the gap.

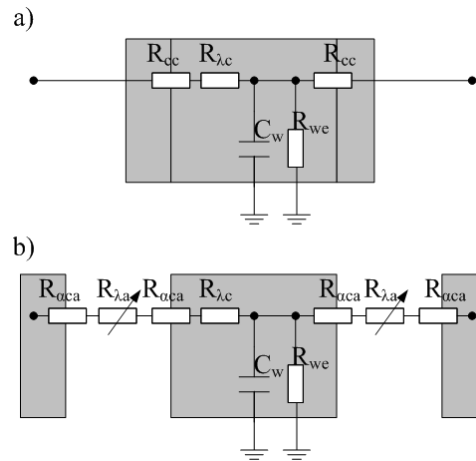


Fig. 6. Detailed thermal network of R_{th} from fig. 5 with a) closed gap, b) open gap

The maximum gap between wedge and copper beam was determined experimentally for the case of the leaf spring by heating and cooling the SMA-actuator and measuring the stroke of the wedge. The results show a hysteresis resulting from the different phase-change-temperatures for heating and cooling which are typical for this type of thermal shape memory alloy. Geometrical considerations result in the following gap dimensions:

$$\text{heating: } l(T) = \begin{cases} 0.41 \text{ mm} & \text{for } T < 45^\circ \text{C} \\ 0.00 \text{ mm} & \text{for } T > 67^\circ \text{C} \end{cases} \quad (1)$$

$$\text{cooling: } l(T) = \begin{cases} 0.41 \text{ mm} & \text{for } T < 23^\circ \text{C} \\ 0.00 \text{ mm} & \text{for } T > 59^\circ \text{C} \end{cases} \quad (2)$$

The thermal resistance resulting from this gap was then derived by heating up the heat source to a certain temperature and then inserting the wedge into the air gap. The distance was adjusted to the 0.41mm the previous examinations yielded. A time constant is then graphically extracted from the heating curve of the wedge and the thermal resistance is calculated according to (3).

$$R = \frac{\tau}{C} = \frac{720 \text{ s}}{21.24 \text{ Ws/K}} = 33.90 \text{ K/W} \quad (3)$$

With the calculated and measured values for the thermal resistances a transfer function $H(s)$ following the scheme of (4) is calculable.

$$H(s) = \frac{\Delta T(s)}{\dot{Q}(s)} = \frac{A}{1-s_1} + \frac{B}{1-s_2} + \frac{C}{1-s_s} \quad (4)$$

With a step function $\dot{Q} = \frac{P}{s}$ as input the transformation back into the time domain yields (5). From this equation the heating power for the cartridge needed to ensure an activated or deactivated state of the leaf spring can be calculated. For $P > 26,2 \text{ W}$ a high enough temperature is ensured and for $P < 0,7 \text{ W}$ the temperature will drop low enough again for

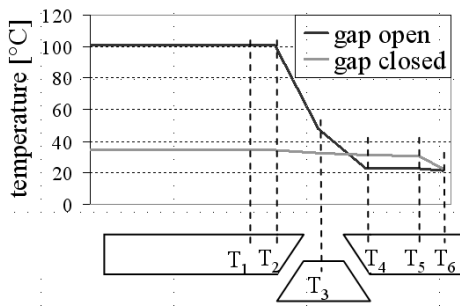


Fig. 7. Temperature profiles for setup with SMA compression spring and conventional tension spring

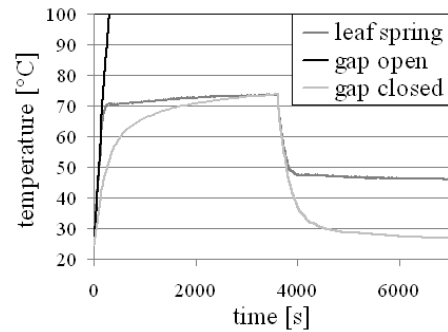


Fig. 8. Temperature for setup with leaf springs in response to a step in input heat

the leaf spring to cool down into the martensitic phase.

$$\Delta T(t) = \frac{P \cdot A}{s_1} (e^{s_1 t} - 1) + \frac{P \cdot B}{s_2} (e^{s_2 t} - 1) + \frac{P \cdot C}{s_3} (e^{s_3 t} - 1) \quad (5)$$

IV. RESULTS AND DISCUSSION

A first experiment was set up with an electrically heated SMA. The heat cartridge provided a thermal flow of 4.95W and the temperature was recorded at six points: T_1 is the temperature of the cartridge, T_2 in the heat source near the gap, T_3 inside the wedge, T_4 and T_5 in the heat sink and T_6 is the temperature of the cooling fluid. Fig. 7 shows the resulting temperature profiles for the uninfluenced (“open”) and the activated (“closed”) case. The temperature difference is rather large with the open gap (80K). In the case of a closed gap the temperatures of source and sink converge and only a gradient of 12K remains. That means that the thermal resistance went down from 16.2 K/W to 2.3 K/W.

The second set of experiments was conducted using the leaf spring directly connected to the heat source. After proving the general feasibility of the proposed mechanism, this experiment was meant to investigate the ability of a self-sensing actuator to regulate the temperature of the heat source. It should prevent overheating by closing the air gap and thereby connecting the heat source to the sink. Additionally it should allow for a fast heating until the targeted temperature. As input a step function with a heat flow of 30W for 3600 seconds and then a drop to 0.7W was applied. The temperature of the heat source was recorded in order to see the effect of the self-regulating thermal flow control. The first run was performed with an open gap (0.41mm), the second one with closed gap and a third one with the leaf spring connected to the heat source. Results are shown in fig. 8. The first run was stopped after reaching 100 °C to prevent the setup from taking damage. With a manually closed gap in a second run a slow heating can be observed. Heat can flow through the beam from the beginning on. With enabled control through the SMA-actuator an intermediate profile was recorded. The temperature climbs steeply until it reaches the temperature for the SMA to change its phase. Then the temperature remains nearly constant as the heat can flow towards the heat sink. After the drop in input heat the temperature of the heat source follows quickly until the

temperature falls below the minimum for the SMA. Then the decline slows down because the gap opens again, interrupting the heat flow towards the sink.

V. CONCLUSION

The two presented setups have demonstrated encouraging results in controlling the thermal resistance actively as well as self-sufficiently using thermal shape memory alloys. A passive cooling mechanism connecting a component to a thermal storage upon reaching a certain temperature was verified in experiments. By integrating a mechanism derived from this foundation into real machining structures the transient thermal behavior can be improved. In combination with a thermal storage based on phase change materials this will lead to a reduced fluctuation in temperature and therefore to increased machining accuracy.

ACKNOWLEDGMENT

The authors would like to thank the German Research Foundation (DFG) for financial support within the SFB/Transregio 96 special research centre.

REFERENCES

- [1] S. Nestmann, “Mittel und Methoden zur Verbesserung des thermischen Verhaltens von Werkzeugmaschinen,” in *Mechatronik: Optimierungspotenzial der Werkzeugmaschine nutzen. Seminarberichte*, 2006, pp. 3.1–3.29. [Online]. Available: <http://publica.fraunhofer.de/documents/N-51905.html>
- [2] K. Jacob, *Ein Beitrag zum thermisch-gerechten Gestalten von Werkzeugmaschinen am Beispiel der Einständer-Koordinaten-Bohrmaschine*, 1981.
- [3] W. Schäfer, *Steuerungstechnische Korrektur thermoelastischer Verformungen an Werkzeugmaschinen*, ser. Berichte aus der Produktionstechnik. Shaker, 1993.
- [4] J. S. Chen, J. Yuan, and J. Ni, “Thermal error modelling for real-time error compensation,” *The International Journal of Advanced Manufacturing Technology*, vol. 12, pp. 266–275, 1996, 10.1007/BF01239613. [Online]. Available: <http://dx.doi.org/10.1007/BF01239613>
- [5] R. Neugebauer, P. Blau, C. Harzbecker, and D. Weidlich, “Ressourceneffiziente Maschinen - und Prozessgestaltung,” in *Zerspanung in Grenzbereichen. 5. Chemnitzer Produktionstechnisches Kolloquium, CPK 2008. Tagungsband*, 2008, pp. 49–67.
- [6] B. Kuhrke, “Ansätze zur Optimierung und Bewertung des Energieverbrauchs von Werkzeugmaschinen,” in *Energieeffiziente Werkzeugmaschinen. Tagungsband*, E. Ebele (PTW Darmstadt) and VDW Frankfurt (M.), Eds. METAV Düsseldorf, 2010.
- [7] S. Nestmann, “Energieeinsparung ohne Genauigkeits- und Produktivitätsverlust,” *wt Werkstattstechnik online*, vol. 102, no. 1/2, pp. 43–44, 2012.

- [8] H. Mehling and L. Cabeza, *Heat and Cold Storage with PCM: An Up to Date Introduction Into Basics and Applications*, ser. Heat and Mass Transfer. Springer, 2008.
- [9] X. Py, R. Olives, and S. Mauran, "Paraffin/porous-graphite-matrix composite as a high and constant power thermal storage material," *International Journal of Heat and Mass Transfer*, vol. 44, no. 14, pp. 2727 – 2737, 2001.
- [10] F. Aggogeri, A. Merlo, and M. Mazzola, "Multifunctional structure solutions for ultra high precision (uhp) machine tools," *International Journal of Machine Tools and Manufacture*, vol. 50, no. 4, pp. 366–373, 2010. [Online]. Available: <http://dx.doi.org/10.1016/j.ijmachtools.2009.11.001>
- [11] M. Mertmann, *NiTi-Formgedächtnislegierungen für Aktoren der Greifertechnik: Funktionelle Eigenschaften und Optimierung*, ser. Fortschritt-Berichte: Grund- und Werkstoffe, Kunststoffe. VDI-Verlag, 1997.
- [12] B. Kim, M. G. Lee, Y. P. Lee, Y. Kim, and G. Lee, "An earthworm-like micro robot using shape memory alloy actuator," *Sensors and Actuators A: Physical*, vol. 125, no. 2, pp. 429 – 437, 2006.